In Vivo Phosphorylation of Histone H1 Variants during the Cell Cycle[†]

Heribert Talasz,* Wilfried Helliger, Bernd Puschendorf, and Herbert Lindner

Institute of Medical Chemistry and Biochemistry, University of Innsbruck, Innsbruck, Austria

Received August 14, 1995; Revised Manuscript Received November 6, 1995[⊗]

ABSTRACT: In vivo phosphorylation of the five histone H1 variants H1a−H1e including $H1^0$ in NIH 3T3 mouse fibroblasts was examined during the cell cycle by using a combination of HPLC techniques and conventional AU gel electrophoresis. Phosphorylation starts during the late G1 phase and increases throughout the S phase. In the late S phase, the H1 variants exist as a combination of molecules containing 0 or 1 (H1a, H1c), 0−2 (H1d), or 0−3 (H1b, H1e) phosphate groups with a share of unphosphorylated protein ranging between 35% and 75%, according to the particular subtype. Pulse−chase experiments show that phosphorylation during the S phase is a dynamic phosphorylation process with a limited phosphorylation maximum. In most H1 subtypes, phosphorylation occurs very rapidly at the G2/M transition with only small amounts of intermediate phosphorylated molecules. Phosphorylation of mouse H1c, however, occurs stepwise during this transition. Phosphorylated mouse histone subtypes from cells in mitosis contain four phosphate groups in the case of H1a, H1c, and H1e and five in the case of H1b and H1d. Comparison of the mouse phosphorylation pattern to that in rat C-6 glioma cells showed differences for H1e and H1d. By comparing the different phosphorylation patterns of the individual H1 variants during the cell cycle, we were able to classify the H1 histones into subtypes with low (H1a, H1c, $H1^0$) and high (H1b, H1d, H1e) phosphorylation levels.

The H1 histones present in a typical cell can be resolved in $H1^0$ histone (Yasuda et al., 1986) and a heterogeneous group of at least five different subtypes with closely related but nonetheless different primary structures (Kinkade & Cole, 1966; Kinkade, 1969; Rall & Cole, 1971). H1 histones bind to the nucleosome core particle, sealing the DNA entry and exit points. The histones consist of a globular central domain flanked by lysine-rich amino-terminal and carboxy-terminal tails (Van Holde, 1988). The central domain appears to interact with the nucleosome core particle, while the positively charged tails interact with the linker DNA and seem to be important in condensation (Allan et al., 1980; Staynov & Craine-Robinson, 1988). Posttranslational phosphorylation of these tails is associated with cell growth and division and may promote the dynamic changes in chromatin structure required for nuclear function (Balhorn et al., 1972a,b; Gurley et al., 1975, 1978; Roth & Allis, 1992). Phosphorylation of H1 histone is enhanced in rapidly dividing cells and diminished in nonproliferating or quiescent cells. During the cell cycle, phosphorylation begins in the late G1 phase and increases throughout the S and G2 phases. During late G2 and mitosis, phosphorylation of H1 subtypes becomes maximal and decreases sharply thereafter (Bradbury et al., 1973, 1974). These cell cycle-related H1 histone modification changing levels imply that H1 modulates chromatin condensation and decondensation, because in vitro studies suggest that electrostatic interaction between H1 and DNA plays a dominant role in chromatin folding (Clark & Kimuram, 1990). In the past few years, the characterization of various cyclin proteins and $p34^{cdc2}$ kinase homologues (Murray & Kirschner, 1989) has increased the importance of phosphorylation of H1 histones, which serve as important in vitro substrates for cdc2 kinase, with phosphorylation occurring exclusively in the tail domains at conserved motifs (Langan et al., 1989). Therefore, it would be of great interest to know the in vivo phosphorylation pattern of the various H1 variants.

In the past, various methods were used to resolve the H1 subtypes and their phosphorylated forms (Ajiro et al., 1981a). These results evidenced a combination of various H1 histones (Ajiro et al., 1981b), or an average of phosphate residues per H1 molecule (Matsukawa et al., 1985). With the combination of reversed-phase high-performance liquid chromatography (RP-HPLC)[1] and conventional AU gel electrophoresis, it is now largely possible to prevent various H1 subtypes phosphorylated to various extents from overlapping and to show the phosphorylation pattern of each subtype. This paper describes for the first time the levels of phosphorylation of each mouse and most rat H1 subtypes during the cell cycle and shows that phosphorylation during the S phase is a dynamic process with a limited phosphorylation maximum rather than a continuous phosphorylation to high levels with a maximum at mitosis. In addition, our results suggest that $H1^0$, H1a, and H1c differ fundamentally from H1b, H1d, and H1e in their mode of phosphorylation during the cell cycle. When comparing the phosphorylation patterns of mouse and rat H1 histone variants, we found these two mammalian species differ in the maximum phosphorylation levels of some corresponding H1 histone subtypes. Furthermore, our results for the maximally phosphorylated murine H1 variants during mitosis were compared with very

[†] This work was supported by the Dr. Legerlotz-Stiftung.

* Correspondence should be addressed to this author at the Institute of Medical Chemistry and Biochemistry, Fritz-Preglstrasse 3, A-6020 Innsbruck, Austria. Telephone: 0512/507-3522. Fax: 0512/507-2876. E-mail: Heribert.Talasz@uibk.ac.at.

[⊗] Abstract published in *Advance ACS Abstracts,* February 1, 1996.

[1] Abbreviations: FCS, fetal calf serum; DMEM, Dulbecco's minimum essential medium; PBS, phosphate-buffered saline; RP-HPLC, reversed-phase high-performance liquid chromatography; TFA, trifluoroacetic acid; AU/PAGE, acid urea/polyacrylamide gel electrophoresis.

0006-2960/96/0435-1761$12.00/0 © 1996 American Chemical Society

recently published data showing the primary structures of several murine H1 histone proteins (Drabent et al., 1995): with the exception of H1c, the number of S/TPKK motifs corresponds to the maximal number of phosphorylation sites found in our study.

EXPERIMENTAL PROCEDURES

Chemicals. Triton X-100, Tris base, and phenylmethanesulfonyl fluoride were obtained from Serva (Heidelberg, Germany), ethylene glycol monomethyl ether was from Aldrich-Chemie (Steinheim, Germany), and all other chemicals were from Merck (Darmstadt, Germany).

Culture and Synchronization of Cells. NIH 3T3 fibroblasts and rat C-6 glioma cells were grown in monolayer culture and cultivated in DMEM (Biochrom, Berlin, Germany) supplemented with 10% FCS, penicillin (60 μg/mL), and streptomycin (100 μg/ml) in the presence of 5% CO_2. For synchronization, cells were seeded at a density of 1.5×10^6 cells/dish (148 cm^2) and grown for 12 h in normal supplemented DMEM. After this time, cells were washed once with prewarmed PBS and then incubated in DMEM supplemented with 0.1% FCS for 72 h to accumulate the cells in the G0/G1 phase. To release the cells from the G0/G1 phase arrest, fresh medium supplemented with 10% FCS was added. Adding serum to the cells started DNA synthesis after a lag period of 4−6 h, reaching maximum S phase at 16 h where about 95% of the nuclei were labeled (Knosp et al., 1991). At 0, 6, and 16 h after the beginning of restimulation, the cells (5×10^7 cells per time point) were washed once with PBS and collected as G0, late G1, and S phase cells, respectively. To accumulate cells in mitosis, 16 h after restimulation 0.06 μg of Colcemid/mL of medium (Boehringer Mannheim, Mannheim, Germany) was added for additional 4−6 h (Gurley et al., 1978). After the treatment with Colcemid, the cells were collected (mitotic-enriched cells), or the accumulated metaphase cells were selectively dislodged from the monolayer with the mitotic shake-off method (Ajiro et al., 1981a). The cells of each experiment were characterized using flow cytometry and light microscopy. These analyses showed over 90% of the cells to be either in S-phase or in mitosis. Autoradiography was performed only with cells in the G0, G1, and S phases in parallel experiments as described (Knosp et al., 1991).

Labeling Conditions and Isolation of H1 Histones. NIH cells were labeled for 1 h in sodium phosphate-deficient DMEM with carrier-free [^{32}P]orthophosphate (3 mCi/5×10^7 cells per time point, 50 μCi/mL; Amersham) during the G0, G1, S, and M phases of the cell cycle. Thereafter, the reaction was stopped by washing with ice-cold PBS.

In the case of pulse−chase experiments, we incubated S phase cells, 16 h after restimulation with 10% FCS, in lysine-free medium with the addition of L-[4,5-^{3}H]lysine (25 μCi/mL, 85 Ci/mmol, Amersham) for 30 min. After this time or after 4 h of chase with the addition of an excess of not radioactively marked lysine, we isolated the H1 histones. For isolation of H1 histones, the cells were incubated in ice-cold lysis buffer (50 mM Tris, pH 7.5, 25 mM KCl, 1 mM $CaCl_2$, 1 mM $MgCl_2$, 0.25 M sucrose, 50 mM $NaHSO_3$, 10 mM 2-mercaptoethanol, 0.1 mM phenylmethanesulfonyl fluoride, and 0.1% (w/v) Triton X-100] for 5 min and were removed from the dish by a rubber policeman. Nuclei were pelleted at 2500*g* for 15 min at 4 °C and washed with lysis buffer without Triton. Whole histones were isolated from the resulting nuclear preparation by extraction with 1.5 mL of 0.2 M H_2SO_4 per 5×10^7 nuclei at 4 °C for 1 h. The mixture was centrifuged at 10000*g* for 20 min. The supernatant was mixed with 5 volumes of chilled acidified acetone and allowed to stand for 12 h at −20 °C. The precipitate was washed once with acetone, resuspended in water containing 10 mM 2-mercaptoethanol, and freeze-dried (Talasz et al., 1993).

HPLC and Polyacrylamide Gel Electrophoresis. RP-HPLC was performed on a Beckman Model 114M dual-pump system equipped with a Model 165 variable-wavelength UV/VIS and a 421A system controller. The eluent was monitored by the absorbance at 210 nm, and the peaks were recorded with Beckman System Gold software. The freeze-dried proteins were dissolved in water with 0.1% TFA and fractionated on a Nucleosil 300-5 C4 column (12.5 cm × 0.8 cm, 5 μm beads, 300 Å). The H1 histones were eluted with a 35 min linear gradient from 41 to 61% B [solvent A: water containing 10% ethylene glycol monomethyl ether and 0.1% TFA; solvent B: ethylene glycol monomethyl ether (10%)/70% acetonitrile (90%) with 0.1% TFA].

To separate the mouse and rat H1 subtypes, which were unfractionated by RP-HPLC, and to analyze the phosphorylated forms of the different variants, we used a 16 cm or 32 cm AU/PAGE system (15% polyacrylamide, 0.9 M acetic acid, and 2.5 M urea) as described by Lennox et al. (1982). The gels were stained with 0.1% Coomassie blue and destained by diffusion. Gels were scanned with a Hirschmann Elscript 440 ATH densitometer, and the distribution of the different bands was calculated with Elscript Evaluation Software version 4.0. Processing of autoradiography and fluorography was performed as described (Knosp et al., 1991).

RESULTS

Preparation of the Various Phosphorylated Mouse and Rat H1 Histone Subtypes. To investigate the in vivo phosphorylation of individual H1 subtypes during the cell cycle, we synchronized the cells to obtain cells from G0 (as a marker of unphosphorylated subtypes), late G1, late S phase, and mitosis. In a first step, we fractionated the whole histones by RP-HPLC and designated the resulting subtypes and subfractions to the Lennox nomenclature (Lennox et al., 1982) using two types of gel electrophoresis and amino acid analysis, as previously described (Lindner & Helliger, 1990; Lindner et al., 1990). In mouse fibroblasts, we found histones H1a, H1b, H1c, and $H1^0$ as pure subtypes, whereas one subfraction was a mixture containing the variants H1d and H1e. In rat C-6 glioma cells, we found histones H1b, H1e, and $H1^0$ as pure subtypes, while histones H1c and H1d were unresolved from each other. It should be noted in this context that the rat glioma cell line lacks the histone variant H1a (Talasz et al., 1993).

In the subsequent AU gel electrophoresis, we analyzed the degree of phosphorylation of the various pure and mixed H1 subfractions obtained by HPLC. Balhorn (Balhorn et al., 1971; Balhorn & Chalkley, 1975) showed that the introduction of phosphate groups into H1 histone results in predictable and readily observable shifts in their mobility in long AU gels. The shifts in mobility can be directly interpreted in terms of the stoichiometry of phosphorylation of individual H1 histone subtypes during the cell cycle. The

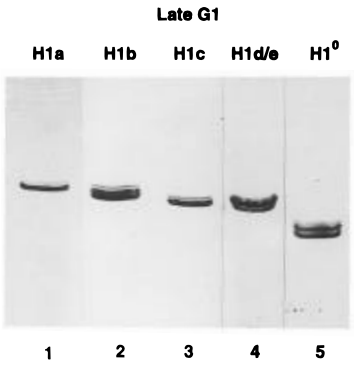

FIGURE 1: Phosphorylation of mouse H1 histone variants during the late G1 phase. Coomassie blue stained AU gel of all five H1 subtypes and $H1^0$ from cells in the late G1 phase. The lowest bands in each lane are always the unphosphorylated forms. Lane 1: unphosphorylated and monophosphorylated H1a. Lane 2: non- to diphosphorylated H1b. Lane 3: unphosphorylated and monophosphorylated H1c. Lane 4: the lowest band represents unphosphorylated H1e, the middle band is a mixture of unphosphorylated H1d and monophosphorylated H1e, and the upper band is monophosphorylated H1d. Lane 5: the lowest band is unphosphorylated $H1^0$b; the middle band is unphosphorylated $H1^0$a and monophosphorylated $H1^0$b, and the upper faint band is monophosphorylated $H1^0$a.

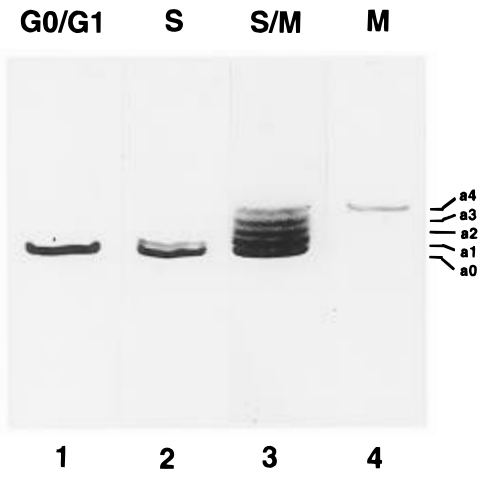

FIGURE 2: Phosphorylation of mouse histone H1a during the cell cycle. Coomassie blue stained AU gel of mouse histone H1a. Lane 1: unphosphorylated H1a from cells in G0/G1. Lane 2: unphosphorylated (lower band) and monophosphorylated H1a from S phase cells. Lane 3: unphosphorylated to tetraphosphorylated H1a histones from mitotically enriched cells designated a0−a4. Lane 4: tetraphosphorylated H1a from pure mitotic cells.

introduction of phosphate groups into the H1 molecule results in the occurrence of additional bands decremented in mobility in successive steps (Langan, 1982). This means that each additional band decremented in mobility represents a H1 protein with one further additional phosphate group.

In Vivo Phosphorylation of Individual Mouse Histone H1 Subtypes. As an example of early H1 histone phosphorylation from cells in the late G1 phase, we compared all five H1 subtypes and $H1^0$ from mouse NIH fibroblasts (Figure 1). In late G1, all H1 subtypes, with the exception of H1b, show mostly unphosphorylated and only few monophosphorylated proteins. This is clearly seen from the H1a and H1c subtypes, whose prominent lower band is the unphosphorylated form and the faint upper band the monophosphorylated form (Figure 1, lanes 1 and 3). Since histones H1d and H1e were not resolved by RP-HPLC, we had to subject these mixed subfractions to gel electrophoresis (Figure 1, lane 4), and therefore it was difficult to determine the precise state of phosphorylation of the two H1 subtypes. The lowest band in lane 4 unambiguously corresponds to the unphosphorylated H1e, whereas the middle, more prominent, band seems to be a mixture of unphosphorylated H1d and monophosphorylated H1e. As for the upper band, it is likely that it represents monophosphorylated H1d exclusively.

Because of the existence of two different $H1^0$ variants, which were not resolvable by RP-HPLC but clearly separated in AU gels (D'Anna et al., 1981; Piña & Suau, 1987), two prominent bands and one upper very faint band are visible in Figure 1, lane 5. The lower prominent band corresponds to the unphosphorylated $H1^0$b variant, whereas the middle band corresponds to unphosphorylated $H1^0$a and perhaps to monophosphorylated $H1^0$b. The faint upper band seems to represent the monophosphorylated $H1^0$a variant. Histone H1b (Figure 1, lane 2) is phosphorylated up to the level of two phosphates per molecule, represented by two additional bands running above the prominent lowest band which corresponds to unphosphorylated H1b.

In the next step we have investigated the phosphorylation pattern of all H1 subtypes from synchronized mouse fibroblasts in the G0 phase (as a marker of pure unphosphorylated protein), S phase, and mitotis. In Figure 2, mouse histone H1a from the G0 phase (lane 1) shows no phosphorylation, because only one unphosphorylated band is visible, whereas in the S phase (lane 2) H1a exists in the unphosphorylated and monophosphorylated forms. In mitotic-enriched cells (lane 3), one unphosphorylated form (lowest band) and four additional bands are clearly visible. These bands correspond to mono-, di-, tri-, and tetraphosphorylated H1a subtypes. H1a from pure mitotic cells was subjected to electrophoresis, running as a single band in lane 4 corresponding to the tetraphosphorylated subtype.

As shown for mouse histone H1b, unphosphorylated subtypes gained from cells in G0 run as a single band in the Coomassie blue stained gel (Figure 3A, lane 1), and therefore no blackening is visible in the corresponding autoradiography (Figure 3B, lane 1). The introduction of phosphate groups into the mouse H1b molecule during the S phase produces three additional bands decremented in mobility. These bands correspond to H1b subtypes carrying one, two, or three phosphate groups per molecule. The lowest prominent band in Figure 3A, lane 2, corresponds to unphosphorylated H1b (designated b0); the uppermost weakly visible band corresponds to H1b molecules containing three phosphate groups, designated b3 in Figure 3A,B, lane 2. In mitotically enriched cell preparations, a combination of cells in the late S and G2/M phases, we found the unphosphorylated band (lowest band in Figure 3A, lane 3) and five additional bands, which correspond to molecules containing one to five phosphate groups (Figure 3A,B, designated b1−b5). Only a few H1b molecules were in an intermediate phosphorylation state (Figure 3A, lane 3, designated b3 and b4), indicating that mitosis phosphorylation occurs very rapidly. In pure mitotic cells gained by the mitotic shake-off method, the H1b molecules run nearly as a single band; i.e., all H1b molecules were in a fully phosphorylated state containing five phosphate groups per molecule (Figure 3A,B, lane 4).

Figure 4 shows the phosphorylation of mouse subcomponent H1c during the cell cycle. In G0 and early G1, only a single band corresponds to unphosphorylated H1c (Figure 4A,B, lane 1). A second monophosphorylated band occurs during the S phase of the cell cycle (Figure 4A,B, lane 2).

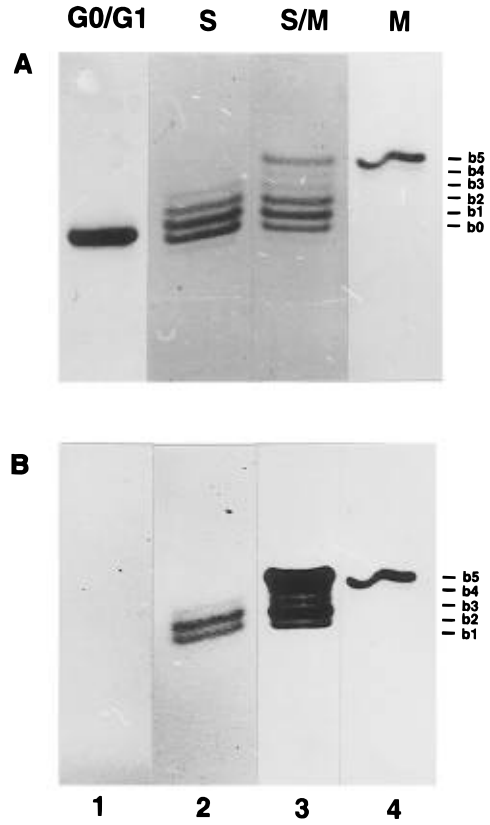

FIGURE 3: Phosphorylation of mouse histone H1b during the cell cycle. Lane 1: unphosphorylated H1b from G0/G1 cells. Lane 2: phosphorylated H1b from S phase cells. Lane 3: Histone H1b from mitotically enriched cell preparations, a mixture of cells from the late S phase and the G2/M phase. The different bands are from bottom to top designated b0−b5, corresponding to unphosphorylated, mono-, di-, tri-, tetra-, and pentaphosphorylated H1b. Lane 4: H1b histone from pure mitotic cells, gained with the mitotic shake-off method. (A) Coomassie blue stained AU gel. (B) Autoradiography of the AU gel from [^{32}P]orthophosphate-labeled histones.

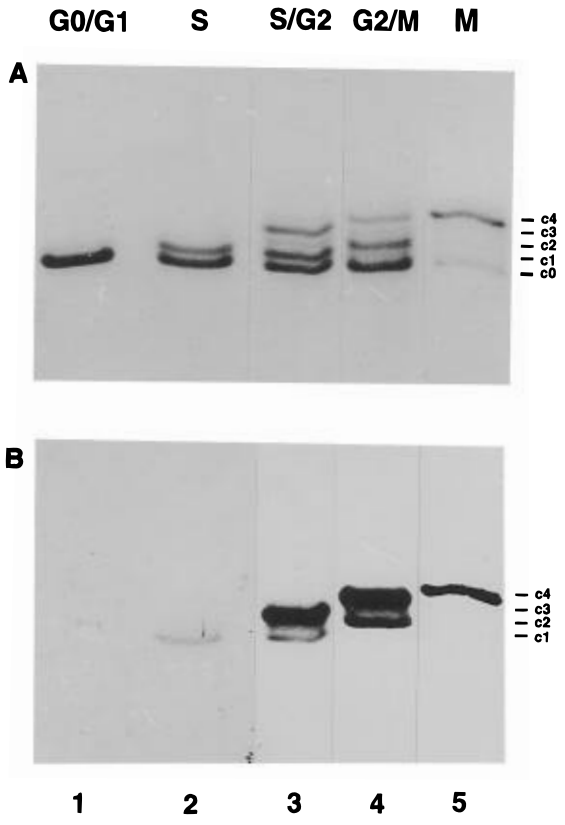

FIGURE 4: Phosphorylation of mouse histone H1c during the cell cycle. Histone preparation from cells of G0/G1 (lane 1), S phase (lane 2), and mitotically enriched cells [4 h of Colcemid treatment (lane 3), and 6 h of Colcemid treatment (lane 4)]. The different bands are from bottom to top: unphosphorylated, mono-, di-, tri-, and tetraphosphorylated H1c designated c0−c4. From cells gained with mitotic shake-off, pure tetraphosphorylated H1c is visible (lane 5). (A) and (B) as in Figure 3.

During the transition from the S to the G2 phase, there exists first an intermediate phosphorylation state with mainly mono- and triphosphorylated H1c molecules (Figure 4A,B, lane 3, designated c1 and c3) and thereafter a state with mainly di- and tetraphosphorylated H1c molecules (Figure 4A,B, lane 4, designated c2 and c4). A pure fraction of mitotic cells shows mainly histone subcomponent H1c phosphorylated to a level of four phosphates per molecule running nearly as a single band (Figure 4A,B, lane 5).

Unfortunately, application of RP-HPLC could not resolve the mouse H1d and H1e variants. Therefore, we collected the peak containing these two variants in G0 and early G1 and obtained two distinctly separate bands on AU gels (Figure 5, lane 1, upper band H1d, lower band H1e). As soon as cells enter the S phase, phosphorylated bands occur, and therefore it is difficult to assign the particular bands to the corresponding H1 subtype. From our results, however, we estimated that during the S phase H1d were phosphorylated to a level of two and H1e to a level of two or possibly three phosphates per molecule (Figure 5A,B, lane 2, designated e1, e2, e3 and d0, d1, d2). When cells cycled from the late S to the G2 and M phases, the mouse histone H1e reached phosphorylation levels of four and H1d of five phosphates per molecule (Figure 5, lane 3). In the mitotic state, both subtypes ran as single bands (Figure 5A,B, lane 4, upper band H1d, designated d5; lower band H1e, designated e4).

H1^0 was separated on RP-HPLC as a single peak; however, on an AU gel, this subtype ran in the unphosphorylated form gained from cells in G0 as two clearly separated bands corresponding to the H1^{0}a and H1^{0}b variants (Figure 6, lane 1, designated a0 and b0). During the late G1 (Figure 1, lane 5) and S (Figure 6, lane 2) phases, each of the H1^0 histones appears in the unphosphorylated and monophosphorylated form, reaching the level of three phosphates per molecule during mitosis (Figure 6, lanes 3 and 4, designated a3 and b3).

Comparison of Rat and Mouse H1 Phosphorylation Patterns during Mitosis. Using rat C-6 glioma cells, we conducted experiments similar to those with mouse fibroblasts. When comparing the same subtype from these two different species, we found differences only in H1d and H1e isolated from mitotic cells (we did not compare H1a). As an example of rat H1 histones prepared from C-6 glioma cells, we used an AU gel to compare the electrophoretic mobility of mouse histones H1d and H1e with that of rat histones H1d and H1e. All other results obtained from rat C-6 glioma cells are summarized in Table 1. In RP-HPLC, rat histone H1e runs as a single peak, whereas H1c and H1d are not resolvable. On AU gels, however, rat H1c and H1d can be clearly separated. Figure 7 shows mouse histones H1d and H1e (lane 1), rat H1e (lane 2), and rat H1c and H1d (lane 3) prepared from mitotically enriched cells. The scans of these three lanes are shown in Figure 8. The unphosphorylated band from both mouse and rat H1e subtypes, designated e0 (Figure 7, lowest band in lanes 1

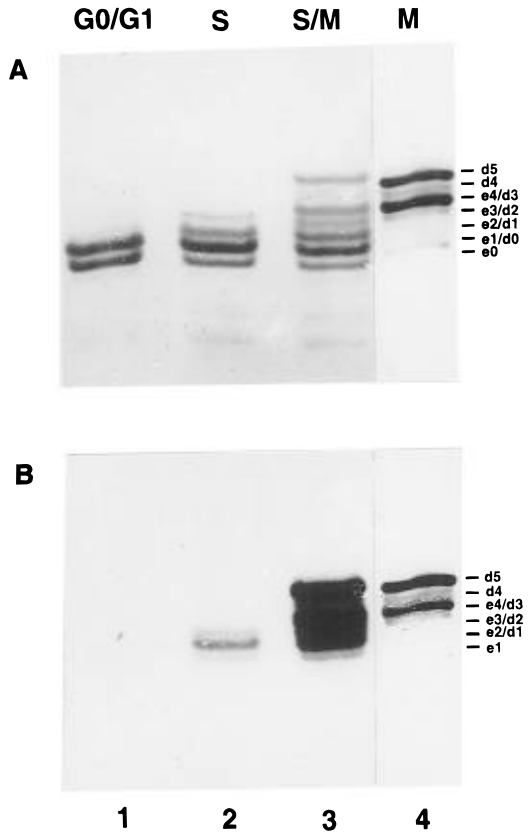

FIGURE 5: Phosphorylation pattern of mouse histones H1d and H1e. G0/G1 (lane 1), S phase (lane 2), and mitotically enriched cells [4 h of Colcemid treatment (lane 3)]. The different bands are from bottom to top: unphosphorylated H1e (e0), combination of monophosphorylated H1e and unphosphorylated H1d (e1/d0), combination of diphosphorylated H1e and monophosphorylated H1d (e2/d1), combination of triphosphorylated H1e and diphosphorylated H1d (e3/d2), combination of tetraphosphorylated H1e and triphosphorylated H1d (e4/d3), tetraphosphorylated H1d (d4), and pentaphosphorylated H1d (d5). Mitotic shake-off (lane 4), only tetraphosphorylated H1e (lower band), and pentaphosphorylated H1d (upper band) are visible. (A) and (B) as in Figure 3.

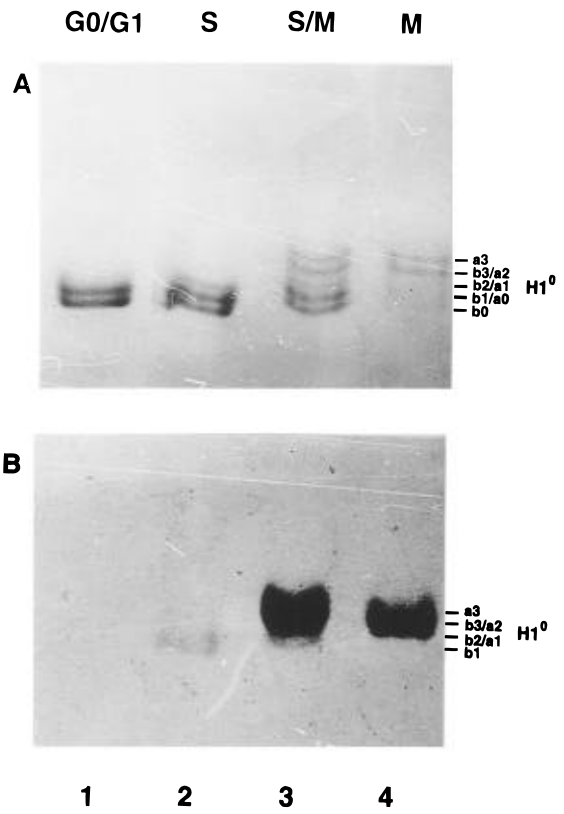

FIGURE 6: Phosphorylation pattern of mouse histone $H1^0$. Lane 1: unphosphorylated $H1^0$a (upper band) and $H1^0$b (lower band). Lane 2: unphosphorylated and monophosphorylated $H1^0$a and $H1^0$b from S phase cells. Lane 3: mixture of un- to triphosphorylated $H1^0$a and $H1^0$b from mitotically enriched cells. Lane 4: triphosphorylated $H1^0$a (designated a3) and $H1^0$b (designated b3) from nearly pure mitotic cells. (A) and (B) as in Figure 3.

Table 1: Maximal Number of Phosphate Groups per Histone Molecule during the G1 and S Phases and Mitosis[a]

	late G1	late S	mitosis
H1a	1	1	4
H1b	2 (2)	3 (3)	5 (5)
H1c	1 (1)	1 (1)	4 (4)
H1d	1 (1)	2 (2)	5 (5/6)
H1e	1 (1)	2/3 (3)	4 (5)
$H1^0$	1	1	3 (3)

[a] Values are numbers of phosphate groups per molecule of histone variants from mouse fibroblasts and from rat glioma cells (in parentheses). The phosphate groups of $H1^0$ from the G1 and the S phase and of H1a are determined only from mouse fibroblasts.

and 2), runs to the same height in the AU gel. Therefore, the phosphorylation patterns are directly comparable. Interestingly, the highest phosphorylation form of rat H1e (Figure 7, lane 2, upper band) is phosphorylated to the level of five phosphates, as compared to mouse H1e at the level of four (Figure 7, lane 1, designated e4). Moreover, rat H1d shows more than the mouse H1d variant's maximum of five phosphates per molecule. The upper two bands in Figure 7, lane 3, correspond to the penta- and hexaphosphorylated rat H1d variant, designated d5 and d6 in Figures 7 and 8.

Pulse and Chase Experiments. Pulse and chase experiments were performed during the late S phase to determine whether H1 histones are phosphorylated immediately after they are synthesized or their net phosphorylation increases more slowly with time after synthesis. NIH 3T3 cells were pulse-labeled with [^{3}H]lysine for 30 min as described under Experimental Procedures. The results are shown in Figure 9A (stained gel) and Figure 9B (fluorography). After 30 min of pulse, the newly synthesized histones are mainly in an unphosphorylated state (Figure 9A,B: lanes 1−3, H1c, H1b, and H1d/e, respectively). At the end of 4 h of chase, even at the end of the S phase, only some of the newly synthesized labeled histones were phosphorylated and shifted to lower migrating bands (Figure 9A,B: lanes 4−6, H1d/e, H1b, and H1c, respectively). We thus assume that H1 phosphorylation is restricted to only a limited portion of the H1 subtype population and we can possibly interpret the limited phosphorylation at the end of the S phase as a dynamic process of phosphorylation and dephosphorylation, in which part of the newly synthesized H1 histones remains unphosphorylated.

DISCUSSION

This paper investigates the dynamic behavior of phosphorylation of the five H1 histone subtypes H1a−H1e including $H1^0$ from mouse fibroblasts and rat C-6 glioma cells and concludes that the individual H1 subtypes vary in the number of phosphate groups per molecule while passing through the cell cycle. Phosphorylation of H1 histones during various cell cycle states has been examined extensively in the past. Whereas the maximum levels of in vitro phosphorylation of the various H1 subcomponents using growth-associated H1 kinase are well-known (Langan, 1982), the in vivo results

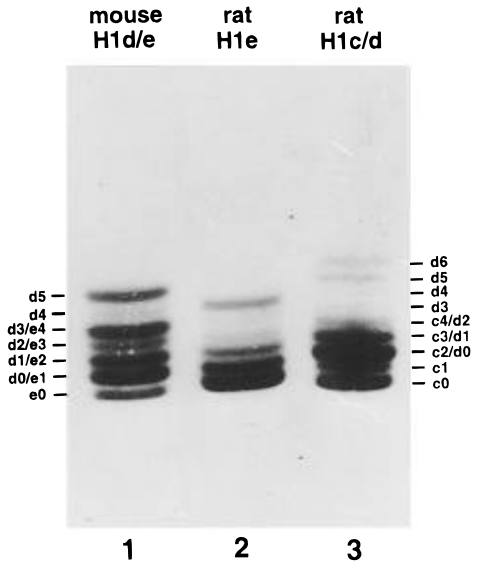

FIGURE 7: Comparison of the phosphorylation pattern of mouse and rat H1 variants in mitotically enriched cells. AU gel from different HPLC fractions of mouse and rat H1 histones from mitotically enriched cells. Lane 1: mouse histones H1d and H1e. e0−e4 means un- to tetraphosphorylated H1e: d0−d5 means un- to pentaphosphorylated H1d. Lane 2: rat histone H1e. Lane 3: rat histones H1c and H1d. c0−c4 means un- to tetraphosphorylated H1c; d0−d6 means un- to hexaphosphorylated H1d.

are incomplete and contradictory (Lennox & Cohen, 1988). The present study, however, compares the H1 phosphorylation pattern of two different mammalian species, providing a more detailed in vivo result.

During the S phase, the H1 subtypes exist as a combination of unphosphorylated and low-phosphorylated forms with one to three phosphates per molecule, with a share of 35−75% of unphosphorylated forms according to the particular variants. This result is in agreement with previous studies (Gurley et al., 1975, 1978) which showed that 40% of the total H1 molecules remain unphosphorylated at late interphase. In rat and mouse H1 variants, the level of three phosphates per molecule was not exceeded during the S phase. The pulse−chase experiments conducted here, which show that even after 4 h of chase in the late S phase only part of the newly synthesized histones are phosphorylated, give rise to the speculation that H1 phosphorylation may occur only at specific sites, i.e., for example, at the sites of the DNA replication fork, and that H1 is dephosphorylated once the replication fork has passed that part of the chromatin occupied by the phosphorylated H1 molecule (Gurley et al., 1975).

At the transition from the S/G2 to the M phase, the H1 subtypes were phosphorylated to higher levels, but only a small amount of intermediate stage phosphorylation was visible at most H1 histone subtypes. Therefore, H1 phosphorylation to higher levels without accumulation of intermediate phosphorylated forms must occur very rapidly. Phosphorylation of H1c during the transition from the G2 to the M phase differed as compared with that of other subtypes. Previous studies have revealed that in both H1b (Lennox et al., 1982) and H1c (Talasz et al., 1993) histones two types of phosphorylation are discernible, resulting in a phosphorylation-induced alteration in protein conformation (Lennox et al., 1982; Jerzmanowski & Krezel, 1986). It may well be that cooperation of the two observed forms of H1c phosphorylation, which occurs stepwise (first mono- and tri-, then di- and tetraphosphorylation), plays a role in the transition from the G2 to the M phase.

Under our in vivo conditions, phosphorylation of each of the H1 subtypes during mitosis reached a well-defined maximum. In contrast to the S phase during mitosis, nearly all molecules of one specific subtype exist as a pure fraction of highly phosphorylated protein. Rat histone H1d, however, has two highly phosphorylated forms with five or six phosphates per histone molecule. This result is in good accordance with the in vitro experiments of Langan (1982), who showed that his fully phosphorylated subcomponent 5 consists of a combination of molecules containing five and six phosphate groups. No additional phosphate was introduced when Colcemid treatment was prolonged, but, instead, the dephosphorylation of highly phosphorylated H1 subtypes began.

Although the five H1 subtypes are phosphorylated to different levels during the cell cycle and differences also exist among some corresponding subtypes from rat and mouse

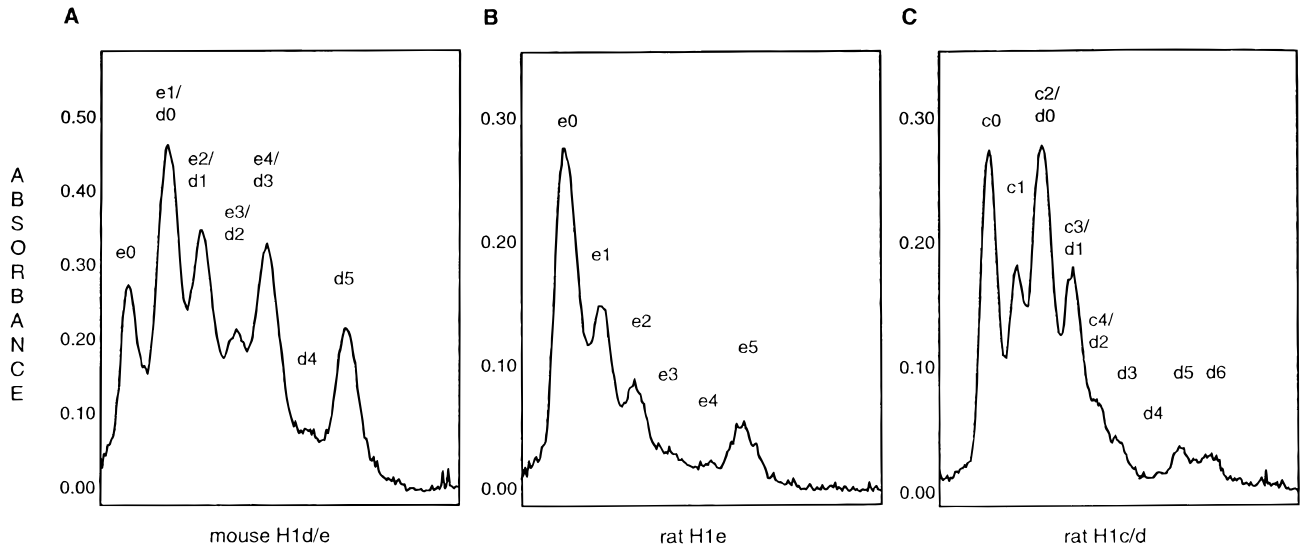

FIGURE 8: Densitometric scans of mitotically enriched mouse and rat H1 variants. Scans from the AU gel shown in Figure 7. Panels A, B, and C are scans from lanes 1, 2, and 3, respectively. Panel A: e0−e4 and d0−d5 mean unphosphorylated to tetraphosphorylated H1e or pentaphosphorylated H1d, respectively. Panel B: e0−e5 means un- to pentaphosphorylated H1e forms. Panel C: c0−c4 means un- to tetraphosphorylated H1c forms, and d0−d6 means un- to hexaphosphorylated H1d forms.

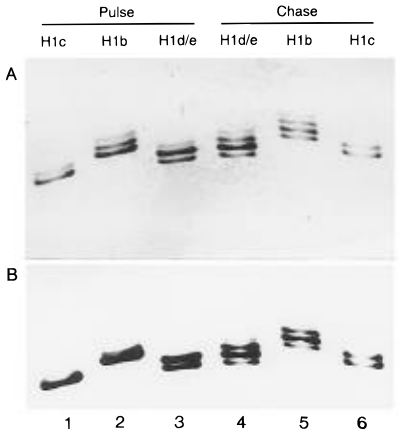

FIGURE 9: Pulse and chase experiment with mouse fibroblasts in the late S phase. Lanes 1−3: H1c, H1b, and H1d/e, respectively. After serum starvation, NIH 3T3 fibroblasts were restimulated for 16 h with medium containing 10% FCS and then pulsed with [^{3}H]lysine in lysine-deficient medium. Lanes 4−6: H1d/e, H1b, and H1c, respectively. In the chase experiment, NIH fibroblasts were pulsed as in lanes 1−3 and then chased for 4 h with an excess of not radioactively marked lysine. (A) Coomassie blue stained AU gel. (B) Fluorography of the AU gel from [^{3}H]lysine-labeled histones.

(H1d and H1e), nevertheless the subtypes show common properties as well. By comparing the various phosphorylation patterns of the individual H1 variants from two species, namely, rat and mouse, we were able to classify the H1 subtypes in two groups. During the S phase, H1a, H1c, and H1^0 histones show a combination of unphosphorylated (60−70%) and monophosphorylated subtypes. Also, during mitosis these subtypes are phosphorylated to a lesser extent than are histones H1b, H1d, and H1e, which during the S phase and mitosis become phosphorylated to higher levels. Thus, it may well be that these phosphorylation characteristics of H1 histones have functional significance.

Very few data are available on rat H1 variant sequences (Drabent et al., 1995), and therefore it was impossible to compare our results for maximal rat H1 phosphorylation during mitosis with the maximal number of so-called growth-related phosphorylation sites (Parseghian et al., 1994). Our results for maximally phosphorylated murine H1 variants during mitosis were, however, confirmed by a very recent paper (Drabent et al., 1995), in which two murine H1 genes were isolated and compared with the nucleotide sequence of all other murine H1 histone genes known. With one exception, these data are in good agreement with the in vivo phosphorylation results presented here. The number of growth-related phosphorylation sites having the SPKK motif or related motifs (TPKK, S/TPAK, TPVK) is four for H1a (Dong et al., 1994), five for H1b (Drabent et al., 1995), three for H1c (Yang et al., 1987), five for H1d (Drabent et al., 1995), four for H1e (Dong et al., 1994), and three for H1^0 (Alonso et al., 1988). Therefore, with the exception of H1c in mitosis, all possible sites with the SPKK motif are phosphorylated. Interestingly, in vivo histone H1c is phosphorylated to the level of four phosphates per molecule during mitosis, whereas only three SPKK motifs are described (Yang et al., 1987). We have no explanation for this difference.

ACKNOWLEDGMENT

We thank A. Devich and Dr. M. Rittinger for their excellent technical assistance and Dr. G. Boeck from the Institute for General and Experimental Pathology, University of Innsbruck, for flow cytometry measurements.

REFERENCES

Ajiro, K., Borun, T. W., & Cohen, L. W. (1981a) *Biochemistry 20*, 1445−1454.
Ajiro, K., Borun, T. W., Shulman, S. D., McFadden, G. M., & Cohen, L. H. (1981b) *Biochemistry 20*, 1454−1467.
Allan, J., Hartman, P. G., Crane-Robinson, C., & Aviles, F. X. (1980) *Nature 288*, 675−679.
Alonso, A., Breuer, B., Bouterfa, H., & Doenecke, D. (1988) *EMBO J. 7*, 3003−3008.
Balhorn, R., & Chalkley, R. (1975) *Methods Enzymol. 40*, 138−140.
Balhorn, R., Riecke, W. O., & Chalkley, R. (1971) *Biochemistry 10*, 3952−3959.
Balhorn, R., Balhorn, M., Morris, H. P., & Chalkley, R. (1972a) *Cancer Res. 32*, 1775−1784.
Balhorn, R., Chalkley, R., & Granner, D. (1972b) *Biochemistry 11*, 1094−1098.
Bradbury, E. M., Inglis, R. J., Matthews, H. R., & Sarner, N. (1973) *Eur. J. Biochem. 33*, 131−139.
Bradbury, E. M., Inglis, R. J., & Matthews, H. R. (1974) *Nature 247*, 257−261.
Clark, D. J., & Kimuram, T. (1990) *J. Mol. Biol. 211*, 883−896.
D'Anna, J. A., Gurley, L. R., & Becker, R. R. (1981) *Biochemistry 20*, 4501−4505.
Dong, Y., Sirotkin, A. M., Yang, Y. S., Brown, D. T., Sittman, D. B., & Skoultchi, A. I. (1994) *Nucleic Acids Res. 22*, 1421−1428.
Drabent, B., Franke, K., Bode, C., Kosciessa, U., Bouterfa, H., Hameister, H., & Doenecke, D. (1995) *Mamm. Genome 6*, 505−511.
Gurley, L. R., Walters, R. A., & Tobey, R. A. (1975) *J. Biol. Chem. 250*, 3936−3944.
Gurley, L. R., D'Anna, J. A., Barham, S. S., Deaven, L. L., & Tobey, R. A. (1978) *Eur. J. Biochem. 84*, 1−15.
Jerzmanowski, A., & Krezel, A. M. (1986) *Biochemistry 25*, 6495−6501.
Kinkade, J. M., Jr. (1969) *J. Biol. Chem. 244*, 3375−3386.
Kinkade, J. M., Jr., & Cole, R. D. (1966) *J. Biol. Chem. 241*, 5790−5797.
Knosp, O., Talasz, H., & Puschendorf, B. (1991) *Mol. Cell. Biochem. 101*, 51−58.
Langan, T. A. (1982) *J. Biol. Chem. 257*, 14835−14846.
Langan, T. A., Gautier, J., Lohka, M., Hollingsworth, R., Moreno, S., Nurse, P., Maller, J., & Sclafani, R. A. (1989) *Mol. Cell. Biol. 9*, 3860−3868.
Lennox, R. W., & Cohen, L. H. (1988) *Biochem. Cell Biol. 66*, 636−649.
Lennox, R. W., Oshima, R. G., & Cohen, L. H. (1982) *J. Biol. Chem. 257*, 5183−5189.
Lindner, H., & Helliger, W. (1990) *Chromatographia 30*, 518−522.
Lindner, H., Helliger, W., & Puschendorf, B. (1990) *Biochem. J. 269*, 359−363.
Matsukawa, T., Adachi, H., Kurashina, Y., & Ohba, Y. (1985) *J. Biochem. 98*, 695−704.
Murray, A. W., & Kirschner, M. W. (1989) *Science 246*, 614−621.
Parseghian, M. H., Henschen, A. H., Krieglstein, K. G., & Hamkalo, B. A. (1994) *Protein Sci. 3*, 575−587.
Piña, B., & Suau, P. (1987) *FEBS Lett. 210*, 161−164.
Rall, S. C., & Cole, R. D. (1971) *J. Biol. Chem. 246*, 7175−7190.
Roth, S. Y., & Allis, C. (1992) *Trends Biochem. Sci. 17*, 93−98.
Staynov, D. Z., & Crane-Robinson, C. (1988) *EMBO J. 7*, 3685−3691.
Talasz, H., Helliger, W., Puschendorf, B., & Lindner, H. (1993) *Biochemistry 32*, 1188−1193.
Van Holde, K. E. (1988) *Chromatin* (Rich, A., Ed.) pp 69−180, Springer-Verlag, New York.
Yang, Y. S., Brown, D. T., Wellman, S. E., & Sittman, D. B. (1987) *J. Biol. Chem. 262*, 17118−17125.
Yasuda, H., Mueller, R. D., Logan, K. A., & Bradbury, E. M. (1986) *J. Biol. Chem. 261*, 2349−2354.

BI951914E